Graefe's Archive for Clinical and Experimental Ophthalmology (2023) 261:339–344
https://doi.org/10.1007/s00417-022-05878-1

RETINAL DISORDERS

Wide-field swept-source OCT angiography (23 × 20 mm) for detecting retinal neovascularization in eyes with proliferative diabetic retinopathy

Takao Hirano[1] · Ken Hoshiyama[1] · Yoshiaki Takahashi[1] · Toshinori Murata[1]

Received: 7 June 2022 / Revised: 26 August 2022 / Accepted: 13 September 2022 / Published online: 28 October 2022

Abstract

Purpose Xephilio OCT-S1 can capture single-acquisition 23 × 20-mm wide-field swept-source optical coherence tomography angiography (SS-OCTA) images and high-resolution images using artificial intelligence. We aimed to evaluate the ability of wide-field SS-OCTA in the detection of retinal neovascularizations (NVs) in eyes with proliferative diabetic retinopathy (PDR).

Methods This retrospective study included 64 eyes of 36 patients (age, 57 ± 10 years; 10 female, 26 male) with PDR. All patients underwent a comprehensive ophthalmological examination, including fluorescein angiography (FA), as well as fovea- and disc-centered 23 × 20-mm OCTA imaging (A-scan/B-scan, 928/807). We compared and examined the number of NV sites identified using conventional methods (merging the findings from biomicroscopy/color fundus photography, FA) and the number of NV sites identified using vitreoretinal interface and superficial retinal slabs of wide-field SS-OCTA images, including the position of NVs (nasal upper, nasal lower, temporal upper, temporal lower, or disc).

Results We identified 168 NVs (32/40/45/35/16, in the abovementioned order) using the conventional method. Fovea-centered 23 × 20-mm OCTA images revealed 162 (96%) NVs (27/39/45/35/16). This method tended to miss nasal NV. In contrast, disc-centered 23 × 20-mm OCTA images identified nearly all NVs, detecting 166 (99%) NVs (32/40/44/34/16) in total. All NVs could be visualized using two wide-field OCTA images: fovea- and disc-centered.

Conclusion Wide-field (23 × 20 mm) SS-OCTA—especially disc-centered—using Xephilio OCT-S1 identified nearly all NVs in eyes with PDR, with a single acquisition, thereby demonstrating its potential clinical application.

Keywords Artificial intelligence · Diabetic retinopathy · Optical coherence tomography angiography · Proliferative diabetic retinopathy · Retinal neovascularization · Swept source

Key messages

- Wide-field (23×20 mm) swept-source optical coherence tomography angiography (SS-OCTA) using Xephilio OCT-S1 identified nearly all retinal neovascularizations (NVs) in eyes with proliferative diabetic retinopathy via a single acquisition, particularlydisc-centered.
- Even in cases wherein NVs were missed, both methods detected at least one NV.
- All NVs were detected using two wide-field OCTA images: fovea- and disc-centered.

Introduction

Neovascularization (NV) in proliferative diabetic retinopathy (PDR) is attributed to high levels of intraocular vascular endothelial growth factor [1, 2] and is commonly observed at the optic disc and mid-periphery [3, 4]. Fluorescein angiography (FA) is the gold standard for the clinical evaluation of retinal vascular alterations, including NV in PDR eyes [5].

Meeting presentation: the content of this paper was presented at the 7th international symposium held by the Asia Pacific Retinal Imaging Society on Aug 20, 2020.

✉ Takao Hirano
takaoh@shinshu-u.ac.jp

[1] Department of Ophthalmology, Shinshu University School of Medicine, 3-1-1 Asahi, Matsu-Moto, Nagano 390-8621, Japan

Although FA is of great importance in PDR management, it requires intravenous dye injection, which may cause nausea and, in rare instances, anaphylaxis [6].

In contrast, optical coherence tomography angiography (OCTA) is an imaging modality based on motion contrast that permits reconstruction of three-dimensional chorioretinal images without dye injection, and therefore can be used in the non-invasive assessment of retinal vascular alterations in patients with PDR [7–9]. However, it is limited by the small size of the scanning area, which is concerning since vascular alterations in PDR extend beyond the posterior pole. Nowadays, with recent advances in software for automatic montage [10, 11] and swept-source (SS) OCTA technology [12, 13], OCTA devices can scan larger fields of view. We previously reported that the NV detection efficacy of montaged SS-OCTA vitreoretinal interface (VRI) slab images acquired by PLEX Elite 9000 (Carl Zeiss Meditec Inc., Dublin, CA) in PDR eyes was comparable with that of fovea-centered FA in the same area of 15×15 mm [12]. A previous study reported that 99.4% of treatment-naïve PDR eyes had NVs in the simulated wide-field SS-OCTA field of view, and some NVs elsewhere (NVEs) were missed completely within this field of view [14]. The abovementioned study suggested that incorporating a simulated SS-OCTA field of view centered on the disc rather than on the fovea could have increased the NV detection rate, and previous treatment with panretinal photocoagulation (PRP) does not affect the detection rate of NVs sites. The Xephilio OCT-S1 (OCT-S1, Canon, Tokyo, Japan), launched in 2019, is an SS-OCT device that can obtain up to 23 mm of wide-field B-scan images [15]. Furthermore, OCT-S1 can capture 23×20-mm wide-field SS-OCTA images in a single acquisition, and produce high-resolution images using artificial intelligence (AI).

In this study, we primarily evaluated the ability of fovea- and disc-centered wide-field SS-OCTA images using OCT-S1 to detect NVs identified using conventional methods, including FA, in eyes with PDR. In addition, whether previous treatment with PRP affected the results was secondarily examined.

Methods

In this retrospective, observational study, we reviewed 73 eyes of 42 consecutive patients aged above 20 years with PDR, diagnosed based on the International Diabetic Retinopathy Severity Scale [16], who visited Shinshu University Hospital between September 2019 and December 2021. All the patients underwent comprehensive ophthalmological examinations, including biomicroscopy/color fundus photography and FA. Eyes with poor-quality images owing to poor fixation, corneal opacity, cataract, preretinal/vitreous hemorrhage, tractional retinal detachment, and a history of vascular endothelial growth factor therapy or vitrectomy were excluded from the study. Data on age, sex, most recent hemoglobin A1c (HbA1c) levels, visual acuity, and prior PRP treatment were collected from medical records. The study was approved by the ethics committee of Shinshu University School of Medicine (approval number: 4908) and adhered to the tenets set forth in the Declaration of Helsinki. Informed consent from patients was obtained by the opt-out method.

The distribution of NVs was first confirmed via conventional methods, i.e., clinical examination and multimodal imaging, including wide-field color fundus photography using CLARUS 500™ (Carl Zeiss Meditec Inc, CA, USA), FA using Heidelberg Retina Angiograph 2 (Heidelberg Engineering, Heidelberg, Germany), and spectral-domain OCT B-scan using Cirrus OCT (Carl Zeiss Meditec Inc, CA, USA). The number of NV sites identified using a VRI slab (from the surface of the internal limiting membrane [ILM] to 2000 μm above the ILM) and a superficial retinal slab (from the surface of the ILM to the posterior of the inner plexiform layer) according to the default settings of the manufacturer's software for both fovea- and disc-centered 23×20-mm OCTA imaging using OCT-S1 (Canon Inc., A-scan/B-scan: 928/807, Fig. 1) were compared with those confirmed by the conventional method. Similarly, for the NV locations (nasal upper, nasal lower, temporal upper, temporal lower, or disc), the OCTA findings were compared with those of the conventional method. Two experienced retina physicians (Y. T. and K. H.), who were blinded to the patient clinical status, identified the NVs using both conventional methods and wide-field SS-OCTA images. If the NVs could not be easily identified using OCTA images of VRI and superficial retinal slabs, the graders were only allowed to extract a slab and review the OCT B-scan to see if it perforates the ILM, which was acquired simultaneously by OCT S-1. The graders considered the NVs to be delineated if the OCTA images demonstrated more than 50% of the size of the NVs identified using conventional methods. In case of discrepancy in the identification of NVs between the graders, they reviewed the images to reach a consensus, and the final grading was used in the analysis. Continuous variables are expressed as mean ± standard deviation. Best-corrected visual acuity (BCVA) results were converted to the logarithm of the minimum angle of resolution (log MAR). A visual acuity of counting fingers was converted to 2, as previously reported [17]. All the analyses were performed using SPSS (version 24.0, IBM, Armonk, NY, USA).

Results

Patient characteristics

Of the 73 eyes reviewed for this study, 9 were excluded from the final analysis owing to poor quality of the FA or OCTA images. Thus, 64 PDR eyes from 36 patients (age: 57 ± 10 years; male, 26; female: 10) were ultimately included in this analysis. All the patients had diabetes mellitus (type 1, 2; type 2, 34), with a mean HbA1c level of 8.2 ± 1.5%.

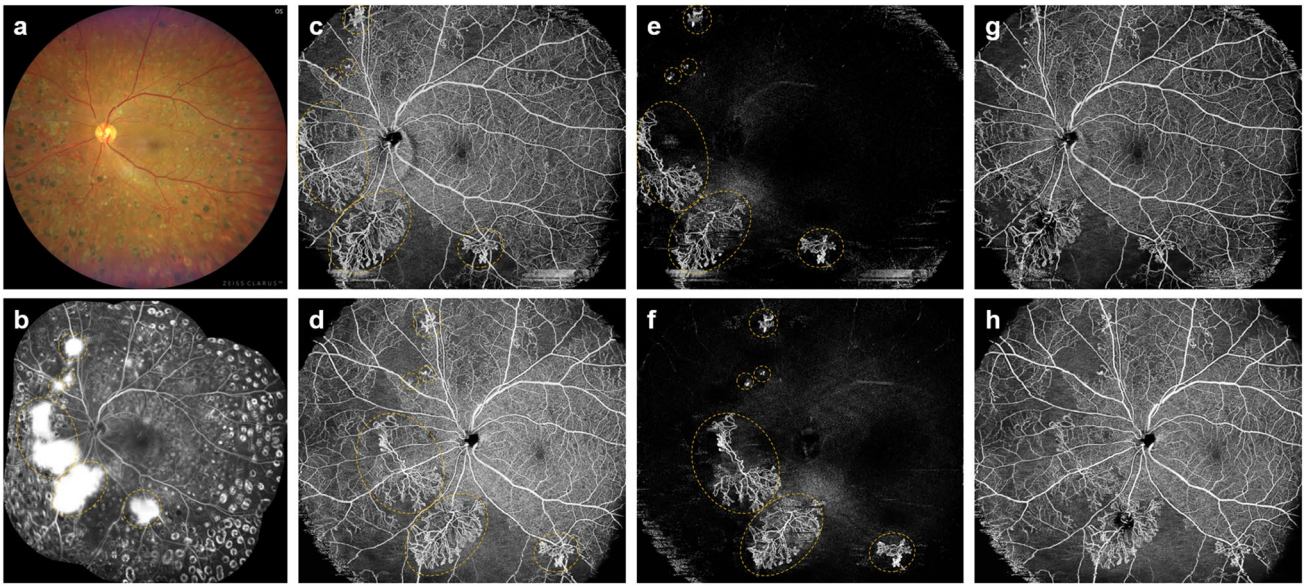

Fig. 1 Wide-field 23 × 20-mm SS-OCTA delineation of NVs identified by conventional methods. Laser scarring by PRP treatment can be observed on wide-field color fundus photography (**a**). Although they are not clearly visible in wide-field color fundus photography, six NVs (orange dashed circle; three, two, and one in the nasal upper, nasal lower, and temporal lower quadrants, respectively) were easily confirmed by dye leakage via montaged FA (**b**). Combined VRI and superficial retinal slabs (from the surface of the ILM to 2000 μm to the posterior of the inner plexiform layer) of fovea- and disc-centered 23 × 20-mm OCTA images depict retinal vascular structures and all six NVs (orange dashed circle), respectively (**c**, **d**). The VRI slab (from the surface of the ILM to 2000 μm above the ILM) of fovea- and disc-centered 23 × 20-mm OCTA images more easily depicts all six NVs (orange dashed circle) in detail (**e**, **f**). Only the superficial retinal slab (from the surface of the ILM to the posterior of the inner plexiform layer) of fovea- and disc-centered 23 × 20-mm OCTA images clearly reveal retinal vessels; although NVs are slightly difficult to identify (**g**, **h**). FA, fluorescein angiography; ILM, internal limiting membrane; NV, neovascularization; OCT, optical coherence tomography; PRP, panretinal photocoagulation; SS-OCTA, swept-source optical coherence tomography angiography; VRI, vitreoretinal interface

The mean duration of diabetes mellitus was 4.4 ± 4.7 years. The log MAR BCVA was 0.28 (approximate Snellen equivalent 20/38) ± 0.54 (range, − 0.18 to 2, approximate Snellen equivalent 20/13 to 20/2000).

Detection of NVs via conventional methods

Conventional methods, such as clinical examination and multimodal imaging without OCTA, were used to identify 168 NVs (NVEs, 152; NV of the disc [NVD], 16) (Table 1). NVEs were detected in the nasal upper, nasal lower, temporal upper, and temporal lower quadrants at 32, 40, 45, and 35 sites, respectively.

Detection of the NVs via wide-field SS-OCTA images

Fovea-centered 23 × 20-mm OCTA images demonstrated 162 NVs (NVE, 146; NVD, 16), equivalent to 96% of the NVs identified by conventional method. This method tended to miss nasal NVs, as NVEs were detected in the nasal upper, nasal lower, temporal upper, and temporal lower quadrants at 27, 39, 45, and 35 sites, respectively. Disc-centered 23 × 20-mm OCTA images identified 166 NVEs (NVE, 150; NVD, 16), equivalent to 99% of the NVs identified by conventional method. This method was able to visualize nearly all the NVs, as the NVEs were detected in the nasal upper, nasal lower, temporal upper, and temporal lower quadrants at 32, 40, 44, and 34 sites, respectively. It was possible to detect all the NVs using two wide-field OCTA images: fovea- and disc-centered. Figure 2 shows a representative case in which a nasal NV that could not be identified with fovea-centered 23 × 20-mm OCTA images was visualized using disc-centered 23 × 20-mm OCTA images. The percentage of eyes in which all the NVs were identified by the conventional method was 92% (59/64 eyes) in the disc-centered OCTA and 97% (62/64 eyes) in the fovea-centered OCTA. The two wide-field OCTA images were able to identify NVs detected by the conventional method in all eyes (64/64 eyes). Both fovea- and disc-centered 23 × 20-mm OCTA images demonstrated at least one NVE, even in cases where individual NVs were missed.

Comparison of wide-field SS-OCTA images between patients with and without PRP treatment

In the group (25 eyes of 13 patients) without a history of PRP treatment, 61 NVs (nasal upper, nasal lower, temporal upper, temporal lower, or disc: 13/17/15/12/4) were identified using the conventional method (Supplemental Table 1). Fovea- and disc-centered 23 × 20-mm OCTA images showed 59 NVs

Table 1 Detection of NV sites by wide-field 23 × 20 mm SS-OCTA as compared with conventional methods

	Nasal upper	Nasal lower	Temporal upper	Temporal lower	Disc	Total
NV sites in fovea-centered 23 × 20 mm OCTA images	27 84%	39 98%	45 100%	35 100%	16 100%	162 96%
NV sites in disc-centered 23 × 20 mm OCTA images	32 100%	40 100%	44 99%	34 100%	16 100%	166 99%
Total NV sites in both fovea- and disc-centered 23 × 20 mm OCTA images	32 100%	40 100%	45 100%	35 100%	16 100%	168 100%
NV sites identified by clinical examination and multimodal imaging	32	40	45	35	16	168

The upper row in each column indicates the number of NV sites, and the lower row indicates the percentage of NVs identified by OCTA

NV, neovascularization; *SS-OCTA*, swept-source optical coherence tomography angiography

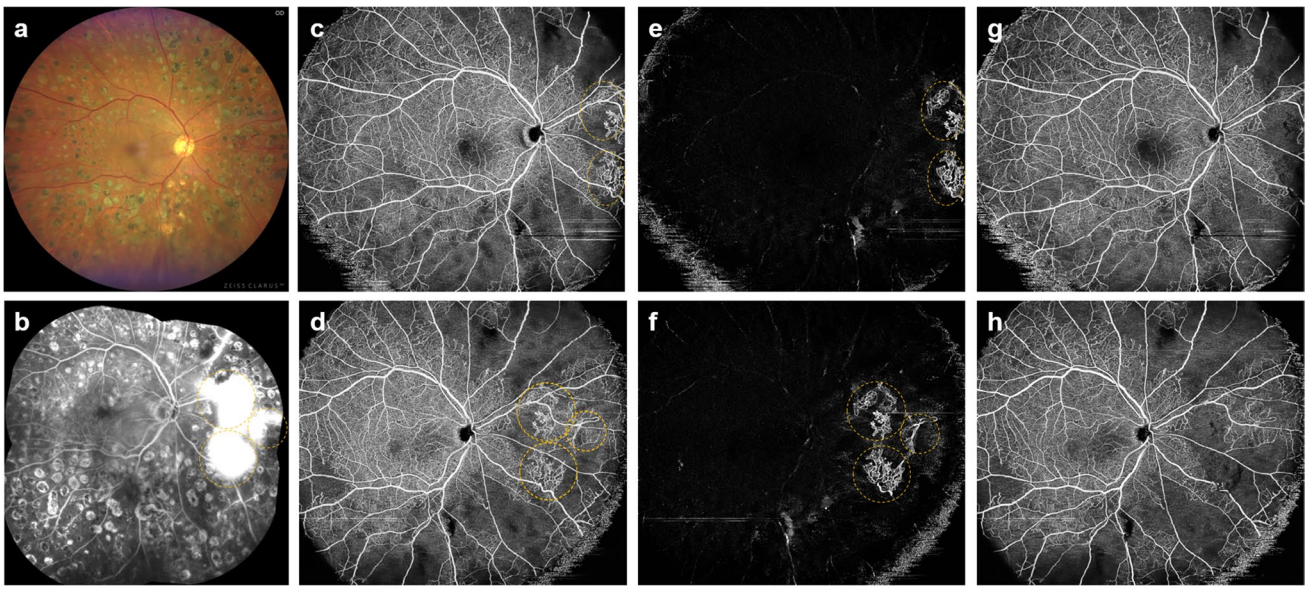

Fig. 2 A case wherein nasal NV that could not be identified using fovea-centered 23 × 20-mm OCTA images was visualized with disc-centered 23 × 20-mm OCTA images. Laser scarring by PRP treatment can be observed on wide-field color fundus photography (**a**). Although they were not clearly visible in wide-field color fundus photography, three NVs (orange dashed circle; one and two in the nasal upper and nasal lower quadrants, respectively) were easily confirmed by dye leakage via montaged FA (**b**). Combined VRI and superficial retinal slabs (from the surface of the ILM to 2000 μm to the posterior of the inner plexiform layer) of fovea-centered 23 × 20-mm OCTA images (**c**) identified two NVs (orange dashed circle) but missed one NV at the nasal lower quadrant. Combined VRI and superficial retinal slabs of disc-centered 23 × 20-mm OCTA images (**d**) depict all three NVs (orange dashed circle). Although the VRI slab of fovea-centered 23 × 20-mm OCTA images missed the nasal lower NVs, the disc-centered 23 × 20-mm OCTA images clearly delineated all the three NVs (**e**, **f**). Only the superficial retinal slab of fovea- and disc-centered 23 × 20-mm OCTA images clearly visualize the retinal vessels; however, the NVs are slightly difficult to identify (**g**, **h**). FA, fluorescein angiography; ILM, internal limiting membrane; NV, neovascularization; OCT, optical coherence tomography; PRP, panretinal photocoagulation; SS-OCTA, swept-source optical coherence tomography angiography; VRI, vitreoretinal interface

(11/17/15/12/4) and 60 NVs (13/17/15/11/4), respectively. In the group (39 eyes of 23 patients) with a history of PRP treatment, 107 NVs (19/23/30/23/12) were identified using conventional methods (Supplemental Table 2). Fovea- and disc-centered 23 × 20-mm OCTA images showed 103 NVs (16/22/30/23/12) and 106 NVs (19/23/29/23/12), respectively. In both groups, it was possible to detect all the NVs using two wide-field OCTA images: fovea- and disc- centered 23 × 20-mm OCTA images; however, both tended to miss nasal NVs.

Discussion

In the present study, we demonstrated that wide-field 23 × 20-mm SS-OCTA images captured by OCT-S1 can reveal nearly all the NVs detected using conventional methods in eyes with PDR.

The OCT-S1 used in this study has two main features. First, it possesses the ability to capture extremely wide OCTA images that are 23 × 20-mm in size, which is the widest area

of any currently marketed instrument. Second, it uses Canon's all-new intelligent denoise feature enabled by AI technology. This denoise processing by AI rapidly improves the image quality of OCTA, and permits a more accurate quantitative evaluation [18, 19]. Hence, OCT-S1 can capture 23 × 20-mm wide-field SS-OCTA images with a single acquisition; moreover, it can capture high-resolution images.

We first examined the detection rate of NVs in eyes with PDR using fovea-centered 23 × 20-mm SS-OCTA images acquired with OCT-S1. Therefore, this method was able to delineate 96% (162/168) of the NVs identified using the conventional method. Although 100% (80/80) of the temporal NVs could be visualized, 8% (6/72) of the nasal NVs were missed. Fovea-centered 23 × 20-mm OCTA images are literally centered on the fovea; thus, the nasal side of the optic disc is inevitably smaller in area than the temporal side. Additionally, a study using color stereo photographs reported that the mean distance from the optic disc to the first NVE site in the nasal upper and nasal lower quadrants was 4.3 mm and 4.8 mm, respectively [3]. These reasons could explain why fovea-centered 23 × 20-mm OCTA images tended to miss nasal NVs. A study using simulated wide-field OCTA images mentioned the possible usefulness of disc-centered OCTA images for better delineating nasal NVs [14]. Following this concept, we investigated the ability of disc-centered 23 × 20-mm OCTA images to detect NVs. As expected, the NV detection rate of disc-centered 23 × 20-mm OCTA images was high (99%, 166/168). However, the NVE detection rate was not 100% for either fovea- or disc-centered OCTA images, although it was possible to identify all the NVEs (100%, 168/168) using both images. Previous reports have shown that 15 × 15 mm SS-OCTA images acquired with PLEX Elite 9000 detected 80.1% and 80.5% of the NV sites identified by ultra-wide-field FA in the treatment-naïve and previously treated eyes, respectively [14]. Compared to the previous finding, the capability of the 23 × 20-mm wide-field OCTA images (whether disc-centered, fovea-centered, or both images) to delineate NVs in this current study is remarkably high. Further evaluation revealed that even in cases where NVEs were missed, both methods detected at least one NVE. PDR is defined by the presence of NV or vitreous/preretinal hemorrhage [16]. Therefore, wide-field 23 × 20-mm SS-OCTA images are useful in the severity-based classification of diabetic retinopathy; they can be used to determine (with 100% accuracy) the presence of NVs via a single, non-invasive examination, although not all the NVs are detected.

Our study has certain limitations that should be considered. First, 8 eyes were excluded owing to low OCTA image quality. Although OCT-S1 has shortened the scanning time by using SS and AI technology, it still takes approximately 10 s to acquire a single image. Patients with PDR with macular damage cannot maintain fixation on a target for a long time; thus, further reduction in the examination time is expected in the future. Second, we previously reported that OCTA images of VRI slabs, which extend anteriorly from the automatically detected retinal surface, are ideally suited for displaying retinal NVs [12]. In this study, VRI slabs were also used to identify NVs; nevertheless, in some cases, determining whether the target vessels extended beyond the ILM to the vitreous was challenging, which required confirmation using OCT B-scan. This is probably because the retinal layer segmentation of OCT-S1 is incomplete. On a busy day, it is difficult to identify NVs by checking both OCTA and OCT B-scan images, and improvement in segmentation is required such that NVs can be identified using only the VRI slab. Third, since OCT-S1 is currently available in Japan and some parts of Europe, Korea, Taiwan, and Singapore, the study population comprised Japanese only. Multi-ethnic studies will be needed to evaluate the usefulness of OCT-S1 across different regions. Finally, this study included eyes that had previously been treated with PRP. OCTA studies have shown that PRP can decrease the size of retinal NV [20]. We had a concern that the presence or absence of PRP would affect our study findings; however, additional investigation demonstrated no marked difference in the NV detection rate with or without PRP. In this study, we examined the presence or absence of NVs, and not the form of NVs; thus, we consider that the history of PRP did not have a significant impact on the results. Despite these limitations, we believe that wide-field 23 × 20-mm SS-OCTA is useful in clinical practice for patients with PDR because it can identify most NVs and at least one NV in a single acquisition, compared with the extended field imaging technique [21] and montaged OCTA images [10], as previously reported. Future studies should be conducted to address this limitation by shortening the testing time and increasing the sample size.

In summary, the wide-field (23 × 20 mm) SS-OCTA identified nearly all the NVs in eyes with PDR via a single acquisition, especially disc-centered. In addition, even in cases wherein NVEs were missed, both methods detected at least one NVE. All the NVs were detected using two wide-field OCTA images: fovea- and disc-centered. Therefore, wide-field (23 × 20 mm) SS-OCTA images appear to be clinically useful in evaluating patients with diabetic retinopathy.

Supplementary Information The online version contains supplementary material available at https://doi.org/10.1007/s00417-022-05878-1.

Author contribution Conceptualization and data acquisition were done by Ken Hoshiyma, Yoshiaki Takahashi, and Takao Hirano. Data analysis and original draft preparation were performed by Takao Hirano and Toshinori Murata. All the authors contributed to the review and editing. All the authors read and approved the final manuscript.

Data availability Data are available upon request.

Declarations

Ethics approval This study was approved by the ethics committee of the Shinshu University School of Medicine (approval number: 4908) and adhered to the tenets set forth in the Declaration of Helsinki.

Consent to participate Written informed consent was obtained from all patients before inclusion in this study.

Consent for publication Not applicable.

Competing interests The authors declare no competing interests.

References

1. Duh EJ, Yang HS, Haller JA, De Juan E, Humayun MS, Gehlbach P, Melia M, Pieramici D, Harlan JB, Campochiaro PA, Zack DJ (2004) Vitreous levels of pigment epithelium-derived factor and vascular endothelial growth factor: implications for ocular angiogenesis. Am J Ophthalmol 137:668–674. https://doi.org/10.1016/j.ajo.2003.11.015
2. Hirano T, Toriyama Y, Iesato Y, Imai A, Murata T (2018) Changes in plasma vascular endothelial growth factor level after intravitreal injection of bevacizumab, aflibercept, or ranibizumab for diabetic macular edema. Retina 38:1801–1808. https://doi.org/10.1097/IAE.0000000000002004
3. Feman SS, Leonard-Martin TC, Semchyshyn TM (1998) The topographic distribution of the first sites of diabetic retinal neovascularization. Am J Ophthalmol 125:704–706. https://doi.org/10.1016/s0002-9394(98)00013-0
4. Fan W, Nittala MG, Velaga SB, Hirano T, Wykoff CC, Ip M, Lampen SIR, van Hemert J, Fleming A, Verhoek M, Sadda SR (2019) Distribution of nonperfusion and neovascularization on ultrawide-field fluorescein angiography in proliferative diabetic retinopathy (RECOVERY Study): report 1. Am J Ophthalmol 206:154–160. https://doi.org/10.1016/j.ajo.2019.04.023
5. Gass JD (1968) A fluorescein angiographic study of macular dysfunction secondary to retinal vascular disease. VI. X-ray irradiation, carotid artery occlusion, collagen vascular disease, and vitritis. Arch Ophthalmol 80:606–617. https://doi.org/10.1001/archopht.1968.00980050608006
6. Kwiterovich KA, Maguire MG, Murphy RP, Schachat AP, Bressler NM, Bressler SB, Fine SL (1991) Frequency of adverse systemic reactions after fluorescein angiography Results of a prospective study. Ophthalmol 98:1139–1142. https://doi.org/10.1016/s0161-6420(91)32165-1
7. Ishibazawa A, Nagaoka T, Yokota H, Takahashi A, Omae T, Song YS, Takahashi T, Yoshida A (2016) Characteristics of retinal neovascularization in proliferative diabetic retinopathy imaged by optical coherence tomography angiography. Invest Ophthalmol Vis Sci 57:6247–6255. https://doi.org/10.1167/iovs.16-20210
8. Hirano T, Kitahara J, Toriyama Y, Kasamatsu H, Murata T, Sadda S (2019) Quantifying vascular density and morphology using different swept-source optical coherence tomography angiographic scan patterns in diabetic retinopathy. Br J Ophthalmol 103:216–221. https://doi.org/10.1136/bjophthalmol-2018-311942
9. Vaz-Pereira S, Morais-Sarmento T, Engelbert M (2021) Update on optical coherence tomography and optical coherence tomography angiography imaging in proliferative diabetic retinopathy. Diagnostics (Basel) 11(10):1869. https://doi.org/10.3390/diagnostics11101869
10. Sawada O, Ichiyama Y, Obata S, Ito Y, Kakinoki M, Sawada T, Saishin Y, Ohji M (2018) Comparison between wide-angle OCT angiography and ultra-wide-field fluorescein angiography for detecting non-perfusion areas and retinal neovascularization in eyes with diabetic retinopathy. Graefes Arch Clin Exp Ophthalmol 256:1275–1280. https://doi.org/10.1007/s00417-018-3992-y
11. Pichi F, Smith SD, Abboud EB, Neri P, Woodstock E, Hay S, Levine E, Baumal CR (2020) Wide-field optical coherence tomography angiography for the detection of proliferative diabetic retinopathy. Graefes Arch Clin Exp Ophthalmol 258(9):1901–1909. https://doi.org/10.1007/s00417-020-04773-x
12. Hirano T, Hoshiyama K, Hirabayashi K, Wakabayashi M, Toriyama Y, Tokimitsu M, Murata T (2020) Vitreoretinal interface slab in OCT angiography for detecting diabetic retinal neovascularization. Ophthalmol Retina 4:588–594. https://doi.org/10.1016/j.oret.2020.01.004
13. Borrelli E, Toto L, Viggiano P, Evangelista F, Palmieri M, Mastropasqua R (2020) Widefield topographical analysis of the retinal perfusion and neuroretinal thickness in healthy eyes: a pilot study. Eye (Lond) 34(12):2264–2270. https://doi.org/10.1038/s41433-020-0804-5
14. Russell JF, Flynn HW Jr, Sridhar J, Townsend JH, Shi Y, Fan KC, Scott NL, Hinkle JW, Lyu C, Gregori G, Russell SR, Rosenfeld PJ (2019) Distribution of diabetic neovascularization on ultra-widefield fluorescein angiography and on simulated widefield OCT angiography. Am J Ophthalmol 207:110–120. https://doi.org/10.1016/j.ajo.2019.05.031
15. Chiku Y, Hirano T, Takahashi Y, Tuchiya A, Nakamura M, Murata T (2021) Evaluating posterior vitreous detachment by widefield 23-mm swept-source optical coherence tomography imaging in healthy subjects. Sci Rep 11:19754. https://doi.org/10.1038/s41598-021-99372-z
16. Wilkinson CP, Ferris FL 3rd, Klein RE, Lee PP, Agardh CD, Davis M, Dills D, Kampik A, Pararajasegaram R, Verdaguer JT, Global Diabetic Retinopathy Project Group (2003) Proposed international clinical diabetic retinopathy and diabetic macular edema disease severity scales. Ophthalmol 110:1677–1682. https://doi.org/10.1016/S0161-6420(03)00475-5
17. Lange C, Feltgen N, Junker B, Schulze-Bonsel K, Bach M (2009) Resolving the clinical acuity categories "hand motion" and "counting fingers" using the Freiburg Visual Acuity Test (FrACT). Graefes Arch Clin Exp Ophthalmol 247(1):137–142. https://doi.org/10.1007/s00417-008-0926-0
18. Kawai K, Uji A, Murakami T, Kadomoto S, Oritani Y, Dodo Y, Muraoka Y, Akagi T, Miyata M, Tsujikawa A (2021) Image evaluation of artificial intelligence-supported optical coherence tomography angiography imaging using oct-A1 device in diabetic retinopathy. Retina 41:1730–1738. https://doi.org/10.1097/IAE.0000000000003101
19. Kadomoto S, Uji A, Muraoka Y, Tsujikawa A (2020) High-contrast scleroconjunctival microvasculature via deep learning denoising. Indian J Ophthalmol 68:2251. https://doi.org/10.4103/ijo.IJO_1079_20
20. Ishibazawa A, Nagaoka T, Takahashi A, Omae T, Tani T, Sogawa K, Yokota H, Yoshida A (2015) Optical coherence tomography angiography in diabetic retinopathy: a prospective pilot study. Am J Ophthalmol 160:35-44.e1. https://doi.org/10.1016/j.ajo.2015.04.021
21. Hirano T, Kakihara S, Toriyama Y, Nittala MG, Murata T (2018) Sadda S (2018) Wide-field en face swept-source optical coherence tomography angiography using extended field imaging in diabetic retinopathy. Br J Ophthalmol 102:1199–1203. https://doi.org/10.1136/bjophthalmol-2017-311358